An Agent-Based Bidding Simulation Framework to Recognize Monopoly Behavior in Power Markets

Ye He [1], Siming Guo [2], Yu Wang [2], Yujia Zhao [2], Weidong Zhu [2], Fangyuan Xu [2], Chun Sing Lai [3,*] and Ahmed F. Zobaa [3,*]

1   Nanjing Vocational Institute of Transport Technology, Nanjing 211188, China
2   Department of Electrical Engineering, School of Automation, Guangdong University of Technology, Guangzhou 510006, China
3   Brunel Interdisciplinary Power Systems Research Centre, Department of Electronic and Electrical Engineering, Brunel University London, Kingston Lane, London UB8 3PH, UK
*   Correspondence: chunsing.lai@brunel.ac.uk (C.S.L.); azobaa@ieee.org (A.F.Z.)

Abstract: Although many countries prefer deregulated power markets as a means of containing power costs, a monopoly may still exist. In this study, an agent-based bidding simulation framework is proposed to detect whether there will be a monopoly in the power market. A security-constrained unit commitment (SCUC) is conducted to clear the power market. Using the characteristics that the agent can fully explore in a certain environment and the Q-learning algorithm, each power producer in the power market is modeled as an agent, and the agent selects a quotation strategy that can improve profits based on historical bidding information. The numerical results show that in a power market with monopoly potential among the power producers, the profits of the power producers will not converge, and the locational marginal price will eventually become unacceptable. Whereas, in a power market without monopoly potential, power producers will maintain competition and the market remains active and healthy.

Keywords: security-constrained unit commitment; power market; locational marginal price; monopoly; Q-learning

1. Introduction

For many years, the power industry has been dominated by large utilities with the authority to manage all generation, transmission, and distribution activities within their operating scope [1]. Such utilities are known as vertically integrated. State-franchised utility companies need a monopoly covering sales and control of the transmission network in an area of operation to generate and transmit electricity in that area. When a residential seller or an independent power producer (IPP) is geographically restricted, the utility is the only buyer [2].

The market structure is slowly transitioning to a more competitive market, the so-called deregulated power market (DPM), owing to a high demand growth coupled with an inefficient system management [3,4]. A DPM encourages electricity suppliers to operate competitively and consumers to choose a preferred power supplier. The United States was the first country to implement electricity deregulation using independent system operators (ISOs), such as ISO New England, NYISO in New York, and the PJM, a regional transmission organization servicing the combined electricity markets of Pennsylvania, New Jersey, and Maryland [5]. Europe is another region where electricity deregulation has been deployed, and the addition of new competitiveness has weakened the traditional monopoly of power utilities, which has had a positive impact on the electricity market [6,7]. Experience has shown that appropriate reform programs in the power sector invariably improve efficiency in terms of cost, service quality, and reliability [8].

In fact, a DPM allows competition among market participants when electricity is traded, but this does not equate to competition. A monopoly reduces the competitive advantage and the positive effects of a DPM. It reduces competition and may generate unreasonable pricing, reducing both the efficiency of the power system and the interests of consumers [9–11]. Market power is the main anti-competitive practice that may hinder competition in the power sector, particularly in the power generation sector [12]. Market power exists in a restructured power system when any single generation company exerts an influence on market pricing or power supply. Market power can be defined as the ability of a seller or a group of sellers to push prices above competitive levels, control total output, or exclude competitors from the relevant market for an extended period of time [12]. It reduces the competitiveness, quality, and impact of technological development. For example, generators with a global market power can manipulate the marginal (spot price) and the locational marginal price (LMP) due to transmission congestion, such as in the Power Pool of England and Wales [13]. Therefore, when there is a monopoly in the power market, the demand from consumers always requires the unit capacity of at least one power producer. This means that the owner of the capacity can keep raising the price or boundary cost to a very high level.

Monopoly recognition for monopoly behavior prevention has attracted attention from researchers for over 10 years. Multiple models are created to recognize the existence of monopolies [14–16]. For example, Yen-Yu Lee et al. in [17] proposed an indicator, the transmission-constrained residual supply index (TCRSI), and generalized the RSI into meshed networks. However, their disadvantage is that they are not comprehensive enough and only consider unidirectional power flow. Another example is that Peng Wang et al. in [18] define must-run generation (MRG) as the minimum capacity that a generator must supply to the system load that takes into account generation and transmission constraints. They believe that when the generator has the potential for monopoly, its MRG value will be greater than zero. These existing studies mainly recognize the 'Must-Buy Section' as the existing condition of monopoly, and thus 'Must-Buy Section' recognition is used as the function of monopoly recognition. Indeed, 'Must-Buy Section' is only a potential condition for monopoly. The non-existence of the 'Must-Buy Section' does not represent the absolute non-existence of monopoly behavior. Thus, a more exact method to recognize the monopoly behavior is required.

In recent years, the demand for the public to understand market mechanisms and how market participants are affected by their results has encouraged the use of simulation models and tools. Some experience has demonstrated the sustainability and efficiency of agent-based system technology in simulating the market behavior of the power market [19]. An agent-based system is a platform that provides agents with the ability to analyze the negotiation context and allows players to automatically adjust their strategic bidding behavior in the market [20,21].

At present, the combination of agent simulation systems and reinforcement learning technology has become a popular research field for analyzing the behavior of market participants in the power auction market [22–25]. In a study of the electricity market, Gong Li and Jing Shi simulated the bidding behavior of suppliers in the electricity market using the Roth Erev learning algorithm [22]. The simulation results show that improving the accuracy of wind forecasts can help increase net revenue for wind power companies. Viehmann et al. use a Q-learning algorithm to analyze the optimal bidding strategy of suppliers. The results show that the prices rise with additional information about the supply-demand ratio only when the number of participants is limited and there is a large asymmetry in size [23]. Ye et al. used the deep Q-learning (DQL) algorithm to study the strategic bidding behavior of producers in the power market [24]. Mohtavipour and Mehdi Jabbari Zideh proposed an iterative collusive strategy search method to detect a collusive strategy in a prisoner's dilemma game in which there is collusive equilibrium. The results show that market participants' collusion in transmission-congested networks can provide them with additional profit opportunities compared to uncongested networks [25]. Nevertheless,

these studies did not consider whether there is a monopoly to reduce competition in the power grid and did not study the behavior-strategy choices of agents further in the case of a potential monopoly in the market.

In this study, we propose an agent-based bidding simulation framework for monopoly identification in the electricity market. In this framework, each electricity producer in the electricity market is modeled as an agent aiming to schedule a bidding strategy for more benefit from electricity trading in power markets. The bidding strategy for each agent is selected from a Q-learning strategy based on the effect of historical strategies, which can be easily replaced by any other preferred strategies. With this framework, monopoly behavior can be recognized by un-converging rising bid prices. If bidding price of all agents converge into a stable range, it means that the monopoly behavior is removed. Unlike the pure monopoly existing from adjustment functions from traditional 'Must-Buy Section' based methods, this framework can also provide a market equilibrium point with behaviors from all agents. Moreover, the effect of behavioral-constraint policies (such as a price upper boundary limit) can be easily simulated in this framework as well. The 'Must-Buy Section' based monopoly recognition model will not be able to obtain this result.

2. The Description of the Proposed Simulation Framework

The typical logic flow of power market trading is revealed below. In the power market, the power generation companies and suppliers submit the quotation curve to the ISO, which obtains the bidding results of each participating party through the scheduling optimization algorithm. The ISO then calculates the LMPs and feeds the winning bid results back to the corresponding power producers [26]. The power producers obtain their winning bid results in the market and calculate their profit. By analyzing historical bidding information and profits, the power producers constantly adjust their quotation curve to obtain greater income in the next bidding round. In this context, the adjustment strategies of different power producers are different, and when developing strategies, their market information is not exactly the same. The profit of each power producer is not only tied to its own bidding price, but it is also affected by what others offer. The power producers' decision-making must be based on the transaction model and algorithm of the trading center (ISO) because a slight strategic change in any company can affect the strategies and earnings of other companies. In a competitive power market, there is a strong correlation between the behavior of different players in the market and their profits. The interests of each participant also depend on the market behavior of other participants in the decision-making process. Figure 1 shows the simulation framework approximating the logic flow above.

Figure 1 shows the proposed agent-based bidding simulation framework. In this framework, it is assumed that the demand is deterministic, power producers have individual generators, and they all bid in the day-ahead market and aim to maximize their profits by using the bidding strategies that best represent their expectations. The scheduling model is an hour-by-hour scheduling optimization that schedules the power generation capacity of power producers at different times of the day in the future. Before participating in the nth bid, each power producer must submit its bid data to an ISO. The bidding data include the unit's quotation curve, generating capacity constraints, startup and shutdown costs, and operating ramping constraints. After collecting the bidding data, the ISO starts the economic dispatch algorithm of the security-constrained unit commitment (SCUC), feeds back the unit output plan of each participating power producer, and calculates the LMPs [26]. Each power producer can obtain the information about their own winning capacity, which supports their bidding strategy in the next bidding iteration.
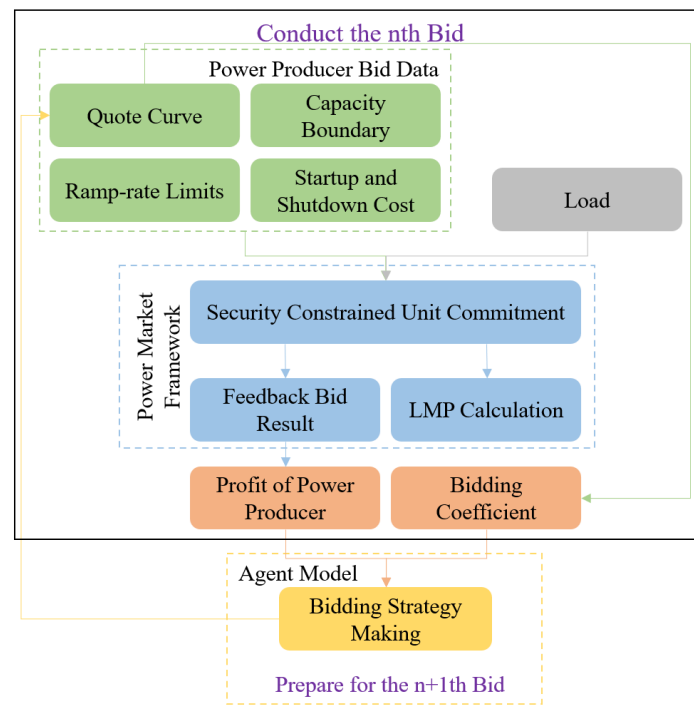
Figure 1. The proposed simulation framework.

In the power market, power producers with monopoly behavior will gradually increase their bidding price, owing to their monopoly capacity, thereby reducing the market's competitiveness. In addition, the agent can fully explore and continue to function autonomously in an environment after being provided with pre-designed behaviors. Therefore, to make the bidding strategies and decisions of power producers smarter, this study assumes that each participating power producer has autonomy and is modeled as an agent that can adjust its bidding strategy according to its own historical bidding information to maximize its own profits.

2.1. The Power Market Framework

2.1.1. The Quote Curve

The unit data submitted by the participating power producers to the ISOs are called bidding data, which indicate the relationship between the output and price of the units of each power producer, as well as the constraints on the output of the units. Equation (1) introduces the quote curve.

$$
\begin{cases}
G_{i,t} = A_i P_{i,t}^2 + B_i P_{i,t} + C_i \\
F(P_{i,t}) = \alpha_{i,t} \cdot G_{i,t}
\end{cases}.
\tag{1}
$$

In Equation (1), $P_{i,t}$ is the output of the ith unit at time period t; A_i, B_i and C_i are the parameters of the generation cost of the ith unit; $G_{i,t}$ is the generation cost of the ith unit at time period t; $\alpha_{i,t}$ is the bidding coefficient of the ith unit at time period t.

2.1.2. The SCUC Model

After receiving the bidding data from the power producers, the ISO obtains the output plan of each unit through the scheduling optimization algorithm. The SCUC model includes UC and transmission network security checks as the base case [27,28]. Equations (2)–(7) reveal the SCUC model:

$$
Min : Obj = \sum_{i=1}^{NG} \sum_{t=1}^{NT} [F_i(P_{i,t}) \cdot I_{i,t} + SU_{i,t} + SD_{i,t}];
\tag{2}
$$

$$\sum_{i=1}^{NG} P_{i,t} = D_t + Loss_t; \tag{3}$$

$$P_{min,i} \cdot I_{i,t} \le P_{i,t} \le P_{max,i} \cdot I_{i,t}; \tag{4}$$

$$\begin{cases} P_{i,t} - P_{i,t-1} \le [1 - I_{i,t}(1 - I_{i,t-1})] \cdot UR_i \\ \qquad\qquad + I_{i,t}(1 - I_{i,t-1}) \cdot UP_i \\ P_{i,t-1} - P_{i,t} \le [1 - I_{i,t-1}(1 - I_{i,t})] \cdot DR_i \\ \qquad\qquad + I_{i,t-1}(1 - I_{i,t}) \cdot DP_i \end{cases}; \tag{5}$$

$$-PL_{max} \le SF \times (KP \times P - KD \times D) \le PL_{max}. \tag{6}$$

Equation (2) is the objective function of power system unit commitment. *NG* is the number of generation units; *NT* is the number of time periods/day; $I_{i,t}$ is the commitment state of unit *i* at time period *t* (binary, 1 means at time period *t* unit *i* is on, and 0 means unit *i* is off); $SU_{i,t}$ and $SD_{i,t}$ are the startup and shutdown costs of the *i*th unit at time period *t*, respectively. Equation (3) reflects the constraints of the supply and the demand balancing. D_t is the total load of the power grid at time *t*, and $Loss_t$ is the transmission loss of the power grid at time *t*. Equation (4) represents the constraint on the unit-generation capacity boundary. P_{min} and P_{max} are the minimum and maximum capacities of the unit reserves, respectively. Equation (5) represents the ramp rate limits of the units, where UR_i and DR_i are the ramp-up and ramp-down rates of the ith unit, respectively, and UP_i and DP_i are the initial ramp-up and ramp-down rates of the ith unit, respectively. Equation (6) represents the load flow boundary constraint [29]. *SF* is the shifting factor matrix, *KP* is the unit correlation matrix, *KD* is the load correlation matrix, $D_{j,t}$ is the size of the *j*th load at time period *t*, and PL_{max} is the upper boundary for the backup power transmission in the transmission line.

2.1.3. The LMP Calculation

The LMP is defined as the marginal cost of supplying the next increment of electrical energy at a specific bus while considering generation and transmission constraints. The electricity market cannot be uniformly cleared when there is congestion in the transmission system. Instead, the market is cleared at the bus level, and the bus clearing price is called the LMP. Physically, the LMP is the cost of supplying the next MW of load at a specific location after considering the costs associated with generation, transmission, and losses [30]. That is, the LMP is the sum of the generation marginal cost, transmission congestion cost, and cost of supplying marginal losses, although the cost of losses is usually small. Equations (7) and (8) reveal a typical solution model of the LMP.

$$\begin{aligned} F = \quad & C_{i,t}P_{i,t} + \lambda \left[0 - 1^T (KP \times P_{i,t} - KD \times D - \Delta L) \right] \\ & + \pi^T \left[SF \times (KP \times P_{i,t} - KD \times D_{i,t} - \Delta L) - PL_{max} \right] \\ & + \pi^{-T} \left[-PL_{max} - SF \times (KP \times P_{i,t} - KD \times D_{i,t} - \Delta L) \right] \\ & + \mu_p^{-T} (P_{i,t} - P_{max}) + \mu_p^{-T} (P_{min} - P_{i,t}) \end{aligned} \tag{7}$$

$$LMP_t = \frac{\partial F}{\partial \Delta L}. \tag{8}$$

The LMP is determined based on the solution of the optimal power flow from the SCUC. In Equation (7), $C_{i,t}$ is the marginal generation cost of the *i*th unit at time period *t*, ΔL is a price-taking incremental bus load, λ is a Lagrange multiplier corresponding to the demand constraint, π^T and π^{-T} are the Lagrange multipliers corresponding to the power flow constraints, respectively, and μ_p^{-T} and μ_p^T are the Lagrange multipliers corresponding to the maximum and minimum generation constraints, respectively. According to the definition of the LMP, it can be calculated using Equation (8).

2.1.4. The Profit of Power Producers

After the SCUC scheduling optimization, the power producers can calculate their profit based on the bidding result.

$$Pro_{i,t} = I_{i,t} \cdot (\alpha_{i,t} - 1) \cdot G_{i,t}. \tag{9}$$

In Equation (9), $Pro_{i,t}$ is the profit of the ith unit at time t. This value is passed to the Q-learning model as an evaluation metric for the Q-learning model.

2.2. The Q-Learning-Based Modelling of Bidding Strategy Making

In the proposed framework, the section of bidding strategy-making is a critical part of the entire simulation. This section actually approximates the market behavior of each power producer, representing their decision-making process with historical bidding information. In this section, the Q-learning-based model is selected as a typical decision-making process. The reason is that the Q-learning-based model is a value-based reinforcement learning algorithm. It finds the optimal action strategy by analyzing historical bidding behavior and its effects. The profit and bidding coefficient of the nth bidding of the power producer are input into the agent model. The sub-state bidding coefficient that is more beneficial to itself is determined through the bidding strategy of the agent in the model and used for the n+1th market bidding. Figure 2 introduces the Q-learning-based model for the bidding strategy making module from Figure 1.
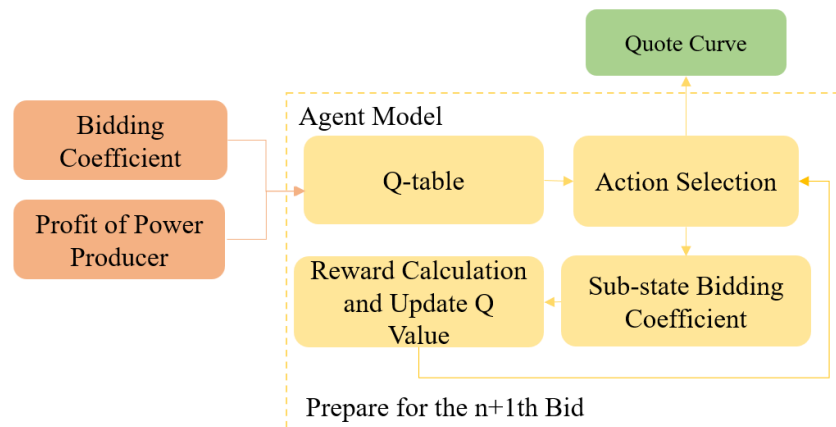

Figure 2. The typical Q-Learning-based model for the bidding strategy making module from Figure 1.

2.2.1. An Overview of the Q-Learning Algorithm

Q-learning is a form of model-free reinforcement learning that works by learning an action-value function that gives the expected result for taking a given action in a given state, following a policy. It provides agents with the capacity to learn to act optimally in Markovian domains by experiencing the consequences of their actions [31]. With the application of the optimal Bellman operator, the state-action value can be obtained through the value iteration in Equation (10).

$$\begin{aligned} NewQ(s,a) = \ & Q(s,a) \\ & + \alpha[R + \gamma \times maxQ\prime(s\prime, a\prime) - Q(s,a)]. \end{aligned} \tag{10}$$

Q-learning comprises the learning agent, environment, states, actions, and rewards. In Equation (10), to implement *Q*-learning, consider $s = [s1, s2, s3, \ldots, s_n]$ as a set of states of the learning agent, $a = [a1, a2, a3, \ldots, a_m]$ as a set of actions that the learning agent can execute, R as the reward or punishment resulting from executing an action a in state s, and α as the learning rate, which is typically set between zero and one. If α is close to zero, the previous knowledge learned becomes more important, whereas if it is close to one, the newly acquired information becomes more relevant instantly. In other words, setting

it to zero prevents the *Q*-table from being updated and therefore prevents any learning. Setting α to a high value, such as 0.9, enables rapid learning. γ denotes the discount factor, which is between zero and one. γ indicates the extent to which the agent's decision-making is influenced by future reward expectations. When γ is close to zero, only the current reward is considered; as γ approaches one, the future reward is given more weight than the immediate reward. $Q(s, a)$ denotes the total cumulative reward gained by the learning agent, and max $Q'(s', a')$ is the maximum Q value of all possible actions a' in the next new state s'. Using Equation (10), an updated *Q*-table, which is shown in Figure 2, is produced.

2.2.2. Action Selection

Arbitrary states of Q-learning are uniquely determined by the bidding coefficients and time ($s_{i,t} = (\alpha_{i,t}, t)$). The agent acts before the next bidding in the market; therefore, the selection strategy is based on historical transaction information, including the data corresponding to the current bidding coefficient and time.

The action taken by the agent is defined by one of three major choices in which the agent decides to execute an action at a quotation below, equal to, or higher than the previous transaction price in the market environment. In this study, the agents learn an action-value function that provides the expected bidding price by selecting an action using an ε-greedy policy approach in a given state. Figure 3 shows the concept of the ε-greedy policy. ε is the exploration rate of Q-learning, which is generally set between 0 and 1. Every time an agent chooses an action, a random number, *rand*, is generated for comparison with ε. When *rand* < ε, the agent selects the action with the largest Q value in the corresponding state; otherwise, it randomly selects any action. This ensures that Q-learning has a breakthrough ability when it encounters a soft boundary.
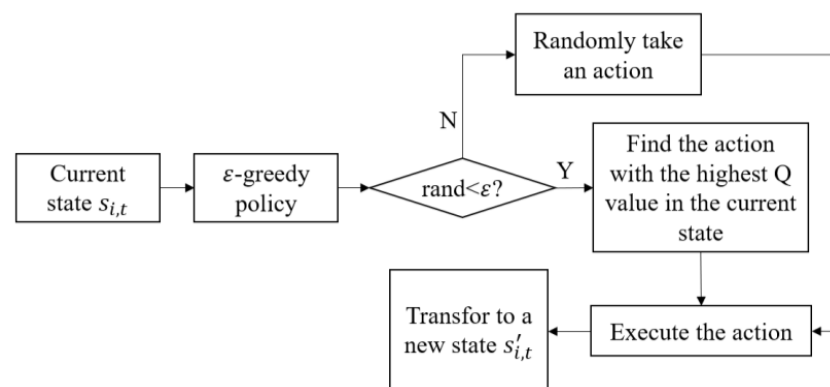

Figure 3. The introduction of ε-greedy policy.

2.2.3. Reward Calculation and Update Q Value

After the agent determines an action, it changes from the current state to another state, so the sub-state bidding coefficient can be obtained according to the current bidding coefficient.

$$\alpha'_{i,t} = \begin{cases} \alpha_{i,t} + A_m & , \quad \alpha_{i,t} < X \\ \alpha_{i,t} & , \quad \alpha_{i,t} \geq X \end{cases} \tag{11}$$

In Equation (11), $\alpha'_{i,t}$ is the sub-state bidding coefficient, A_m is the value obtained by performing the *m*th action, and *X* is the bidding price boundary of the power producer.

The update of the bidding coefficient is accompanied by an update to the quotation curve of the power producer. The updated quotation curve is then sent to the electricity market. After the market is cleared, the power producer can obtain a set of time-series profit value data, which is the feedback value. Therefore, the reward of the environment, $R_{i,t} = Pro_{i,t}$, and the Q value in any state is updated using the following Bellman equa-

tion [32]. Based on this formula, the *Q*-table update for NT periods can be completed:

$$
\begin{aligned}
newQ(s,a) \;=\; & Q(s_{i,t},a) \\
& + \alpha[R_{i,t} + \gamma \times \max Q(s'_{i,t},a\prime) - Q(s_{i,t},a)].
\end{aligned}
\tag{12}
$$

2.2.4. The Simulation Execution Process

A full detailed procedure for simulating Q-learning agents for the proposed bidding simulation framework is provided as follows:

Initialize *Q* value (*Q*(*s*,*a*)) for all state-action pairs.
Repeat (for each episode):

For each time step t:
Given state $s_{i,t}$, take action *a* based on *ε*-greedy policy.
Obtain reward $R_{i,t}$, and reach new state $s'_{i,t}$.
Update *Q*(*s*,*a*) using Equation (12).

3. Numerical Study

3.1. Background

This paper selects a typical 9-bus system and a 33-bus system to verify the feasibility of the proposed scheme. Figure 4 shows the structure of both systems.
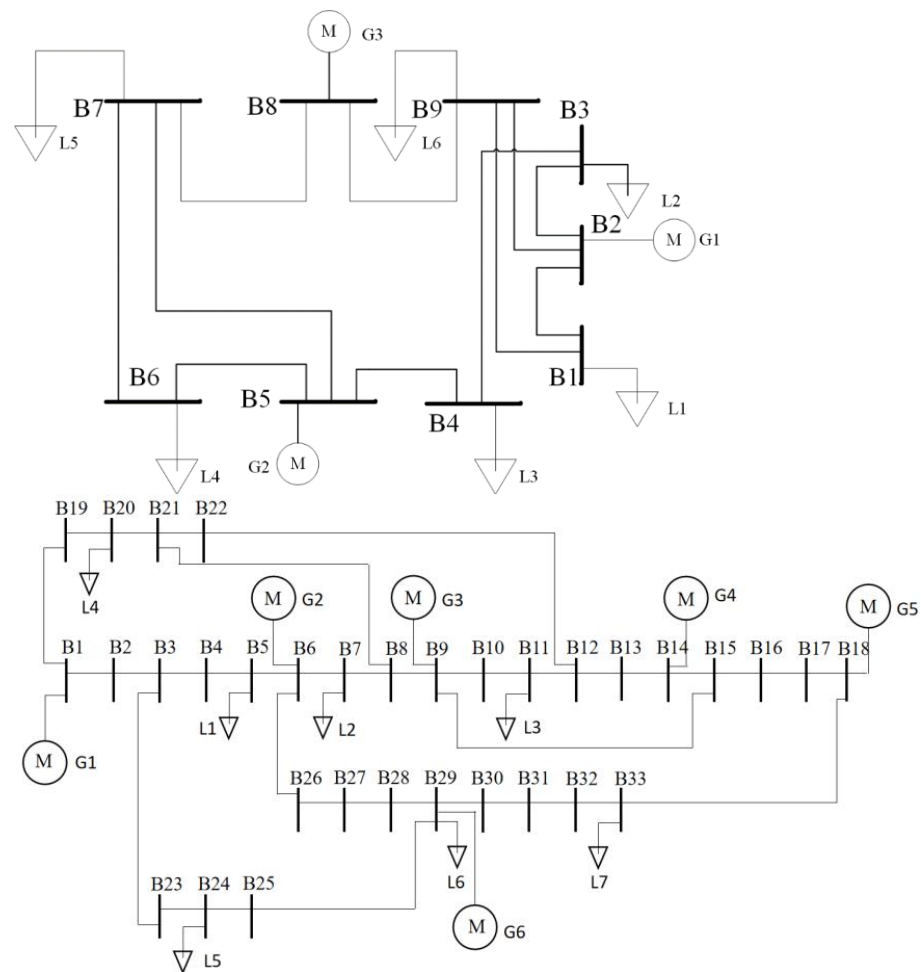

Figure 4. The 9-bus system and the 33-bus system used in the numerical study. (B stands for bus, L stands for load, and G stands for generator).

Each system contains 2 scenarios: one is a case with monopoly and the other is a case without monopoly. The monopoly verification is rechecked by traditional methods in Table 1.

Table 1. Scenarios introduction on both systems.

System	Scenario	Gen NO.	TCRSI Result X Value	MRG Result X Value
9-Bus	SCN 1	Gen No. 2	0.7837580 (Exist)	85.848419 (Exist)
	SCN 2	Gen No. 2	1.008404 (Not Exist)	0 (Not Exist)
33-Bus	SCN 1	Gen No. 1	0.844809 (Exist)	55.110000 (Exist)
		Gen No. 6	0.963207 (Exist)	14.398432 (Exist)
	SCN 2	Gen No. 1	1.142996 (Not Exist)	0 (Not Exist)
		Gen No. 6	1.110499 (Not Exist)	0 (Not Exist)

In Table 2, Gen. NO. 2 stands for No. 2 power producer. The Gen of System exists monopoly when the result value is less than one in TCRSI and more than zero in MGR. In Table 2, the monopoly power producers in the 9-bus and 33-bus systems are listed, and result values of the MRG and TCRSI of the power producers in two different scenarios are also listed. The details of both systems are introduced in Appendix A.

Table 2. Q-learning related parameters.

Item	Value	Item	Value
Action 1	−0.05	exploration rate	0.95
Action 2	0	learning rate	0.1
Action 3	0.05	discount factor	0.9

Table 2 introduces the Q-learning related parameters. Three actions are set by the agent's possible strategies, decreasing, maintaining, and increasing the value of the bidding coefficient. The exploration rate is set to 0.95. The literature suggests that the discount factor (γ) should be set to 0.1, and the learning rate parameter (α) is 0.9 [33].

In this section, two scenarios are selected for the case simulation analysis. In Scenario 1, there is a certain time when the maximum power generation capacity of the two power producers cannot meet the load demand. In Scenario 2, the maximum power generation capacity of any two power producers can meet the load demand at any time. The SCUC problem is formulated using YALMIP in MATLAB and solved using GUROBI 9.5.1. The agents in each scenario of the 9-Bus System and 33-Bus System executed 150,000 sets and 67,000 sets, respectively, and output simulation results every 24 h.

3.2. The Result Analysis of Both Systems

Figure 4 shows the result comparison between scenario 1 and 2 for the 9-bus system. Figure 5 shows the result comparison between scenario 1 and 2 for the 33-bus system. The following features can be revealed in the two comparisons above.

1. Power producers with low power generation costs have the greatest advantage during the early stages of the simulation. They are in an environment where quotations are

raised, profits are rapidly increasing, and they can occupy most of the market share during the long-term simulation process. In the example of the 9-bus system in Figure 5a–d, power producer 1 occupied a large market share in the long-term simulation process, accounting for more than half of the total share. Its profit growth rate was faster than that of other power generation companies at the initial stage, and the profit of power producer 1 reached a higher level than that of the other power producers. In the example of the 33-bus system in Figure 6a–d, compared with other power producers, power producer 1 and 6 had lower costs, so their profits at the beginning of simulation grew rapidly, and they occupied a certain share in the whole simulation process, accounting for approximately one-third of the total shares, respectively.

2. Power producers with low power generation costs must find suitable bidding strategies through long-term games with other power producers to bring profits to their companies. As shown in Figures 5c,d and 6c,d, low-cost power producers, such as power producer 1 in the 9-bus system and power producer 1 and 6 in the 33-bus system, have large fluctuations in their profits in the long-term market simulation. If they cannot find an appropriate bidding strategy, they may have small or even no bid winning volume, leading to lower profits. Therefore, it is very important to find an appropriate bidding strategy.

3. The agent will always choose a strategy that is conducive to increasing interest. In the simulation experiment of Scenario 1, when there is a structured monopoly in the electricity market and the supply and demand balance of the power grid needs to purchase power from a fixed electricity seller, the agent will continue to increase the quotation during the simulation process, and the benefits will continue to increase. Then, there will be other sellers in the market to increase their quotations, and the income of each seller cannot converge, which makes the LMP continue to rise and the market collapses. Thus, the owner of this capacity will keep increasing the price or the claimed boundary cost to a very high level. There may be malicious bidding by producers in the market to drive prices up. As shown in Figures 5e,f and 6e,f, the average electricity price in Scenario 1 is much higher than that in Scenario 2, and the electricity price in Scenario 1 shows a continuous upward trend.

4. In the simulation experiments of Scenario 2, any generation section of any power producer can be replaced by other power producers. Before the optimal bidding strategy is found, the electricity price in the electricity market increases. However, through the strategy selection between the agents, the parties quickly reach convergence, the market tends to be balanced, and it becomes a competitive electricity market. The producers find the optimal quotation strategy in the market environment. As shown in Figures 5f and 6f, the average electricity price in the power market shows a continuous rising trend at the beginning of the simulation, with the 9-bus system increasing approximately one sixth of the initial price and the 33-bus system increasing approximately one fifth of the initial price. Through the strategic choice among agents, all parties reached a consensus quickly, and the market tended to be balanced, becoming a highly competitive electricity market.

5. The successful rate of winning, assuming generation capacity, in the monopoly case is higher than that in the case without monopoly. It can be revealed by the degree of fluctuation in Figures 5a,b and 6a,b. Higher fluctuation in the market share indicates that even competitors with small market power will still obtain chances to win higher generation capacity, which represents a more fair environment in power market. In other words, competition in the case without monopoly is much heavier.

6. The price fluctuation in the case with monopoly is smaller than in the case without monopoly. As shown in Figures 5e,f and 6e,f, after a certain period of simulation, the average price in the case without monopoly fluctuates sharply in a range due to fierce competition among the power producers. The reason for this phenomenon is that more heavy competition in the case without monopoly will lead to more risk in the winning capacity. Thus, the power producers will need to decrease their prices frequently when they face decreasing winning capacity.

Figure 5. (**a**). The market share of all power producers in Scenario 1. (**b**). The market share of all power producers in Scenario 2. (**c**). The profits of all power producers in Scenario 1. (**d**). The profits of all power producers in Scenario 2. (**e**). The average LMP of all buses in Scenario 1. (**f**). The average LMP of all buses in Scenario 2.

(a)

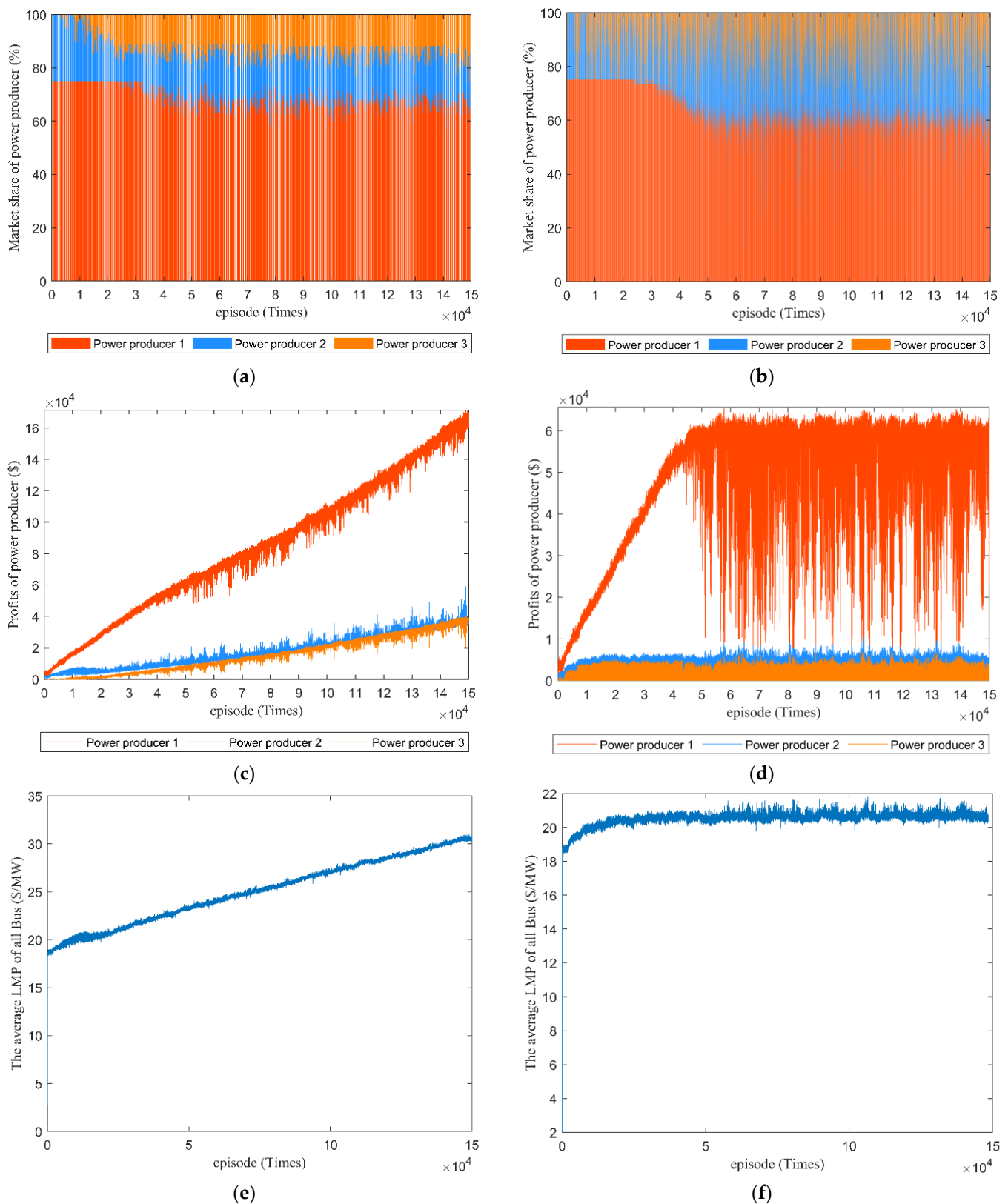(b)

(c)

(d)

(e)

(f)

Figure 6. (**a**). The market share of all power producers in Scenario 1. (**b**). The market share of all power producers in Scenario 2. (**c**). The profits of all power producers in Scenario 1. (**d**). The profits of all power producers in Scenario 2. (**e**). The average LMP of all buses in Scenario 1. (**f**). The average LMP of all buses in Scenario 2.
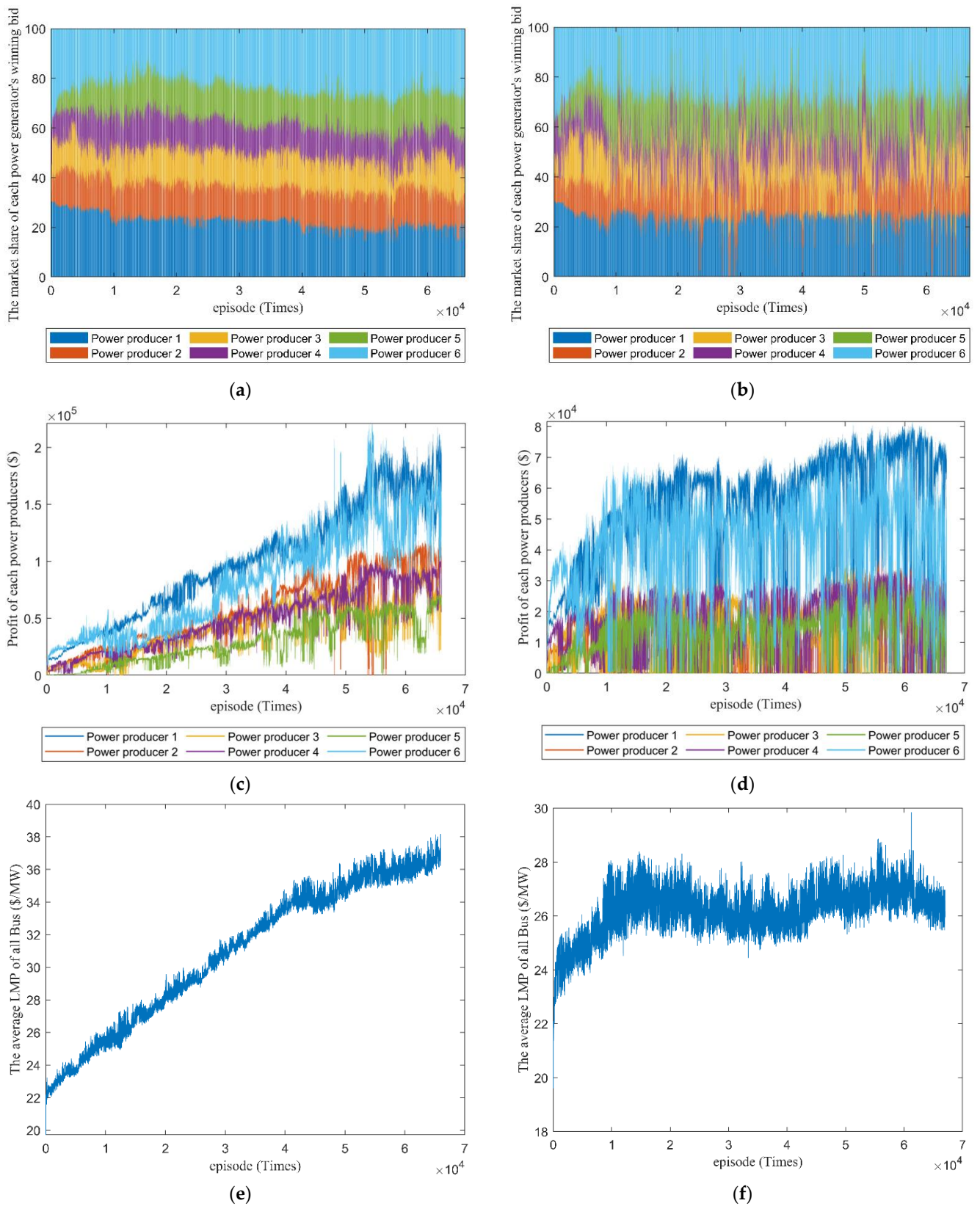
3.3. Result of Hidden Monopoly Recognition and Effect of Price Boundary

To verify the advantages of the proposed scheme compared to the traditional methods, another case on a 6-bus system is selected for simulation. Figure 7 shows this 6-bus system, and its data is in Appendix B. For this 6-bus system, traditional 'Must-Buy Section' based models, such as TCRSI and MRG, recognize that there is no monopoly in it. However, the simulation result in Figure 8a shows that the monopoly behavior exists when bidding prices rise continuously. The reason for this interesting phenomenon is that the two power plants naturally form a grouping monopoly. Indeed, the bid-winning rule of the power market in the simulation performs similar to searching a minimum total cost solution with constraints satisfied. Thus, the winning capacity of all generations actually depends on the relative relationship among prices from generation plants rather than the absolute value of the price. For example, if the two generation plants in the 6-bus system increase 10 USD/kWh simultaneously, the winning capacity of each plant will not change. Thus, when both plants simultaneously increase their bidding price, they will find that their winning capacities have not changed. This signal encourages them to keep increasing their bidding prices and performs similarly to monopoly behavior. Though these two plants do not communicate with each other, this phenomenon shows that they naturally perform similar to a group with simultaneous behavior and form a kind of grouping monopoly. This phenomenon will seldom happen in those cases where there are many competitors, for behavior randomness makes it difficult for simultaneous behavior to occur. However, in cases with small generation groups, such as the case here, the randomness is small, and the probability of this grouping monopoly increases. Moreover, this situation cannot be recognized by traditional 'Must-Buy Section' methods.
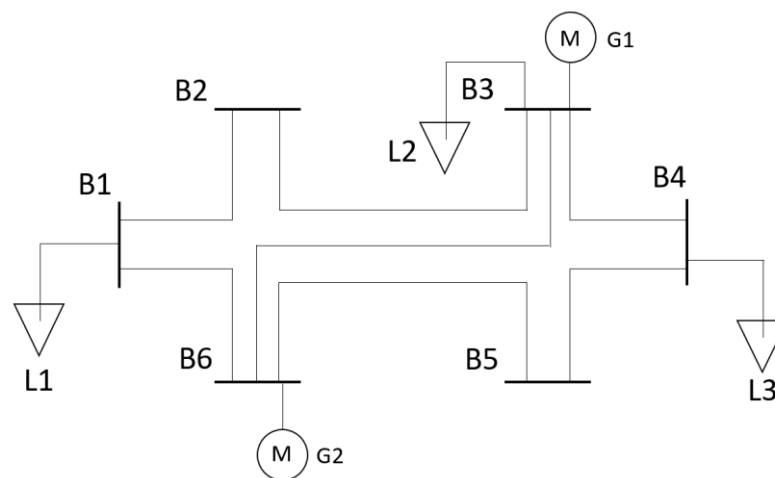
Figure 7. The 6-Bus System used in the numerical study. (B stands for bus, L stands for load, and G stands for generator).

To prevent this phenomenon, one possible way is to set up a price boundary as a constraint to limit the monopoly behavior. The proposed framework can easily simulate the result of the price boundary setting. Figure 8b shows the result of the effect of a price boundary. Once the restrictions are imposed on the power producers, the bidding coefficients of Power producer 1 and 2 cannot rise indefinitely. The bidding coefficient of Power Producer 1 is stable at approximately 1.4, and that of Power Producer 2 is stable at approximately 1.2.

(a)

(b)

Figure 8. (**a**). The bidding coefficients of each power producer with no price boundary. (**b**). The bidding coefficients of each Power producer with a price boundary.

4. Conclusions

This study proposes an agent-based bidding simulation framework to recognize monopolies in power markets. Using the proposed framework, the bidding behavior of electricity producers may change. Changes in the LMP in long-term electricity markets can be simulated to determine whether the electricity market is operating healthily. The results o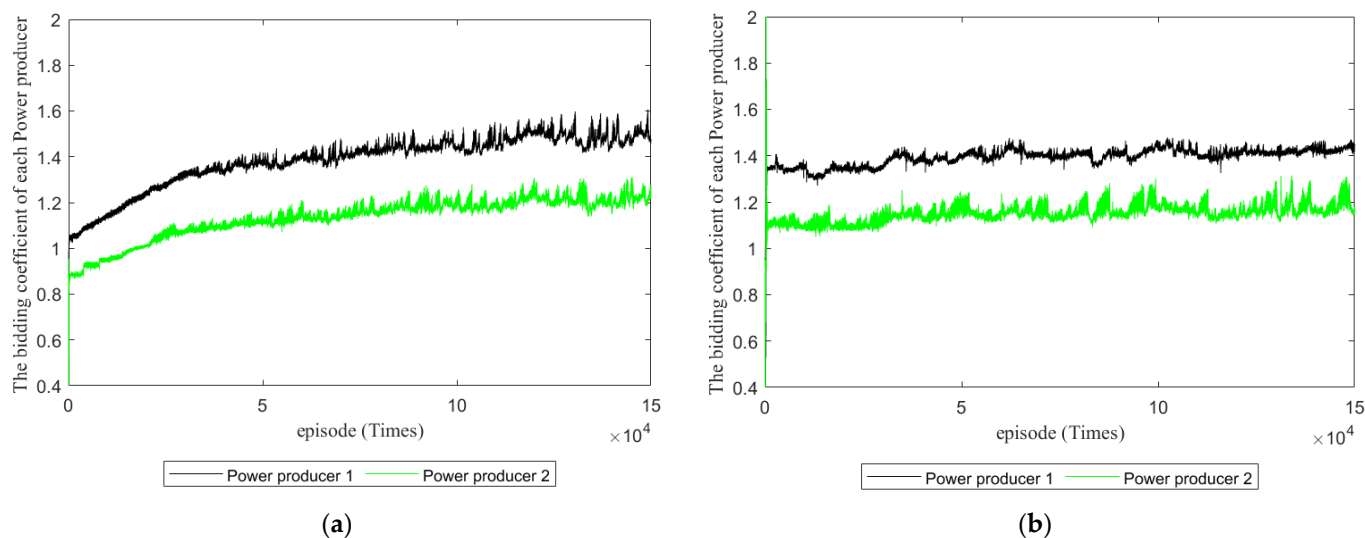f the numerical study on the proposed framework show that in a power market with monopoly potential, the profit of the power producers does not converge, and the market price becomes unacceptable. Whereas in a power market without monopoly potential, power producers maintain competition, and the market remains active and healthy. For the structural design of the electricity market, the proposed framework can become a tool for market monitoring to detect the health of market operations.

Compared to traditional monopoly recognition methods, the largest advantages of the proposed method include three points. The first point is that the proposed framework can reveal the details of the market operation's evolution quantitatively. It not only reveals the existence of monopoly, but also shows the entire performance in the process of monopoly under a given behavior model. The second point is that the proposed framework can be easily used in the simulation of different bidding strategy behaviors by modifying the behavior module without making changes to the other modules, as well as to simulate different market environments by only changing the power market scheme module. This feature enables the proposed framework to be utilized widely in different power market analyses with low cost in modelling and programming. The third point is that the proposed framework can reveal more monopoly cases than traditional 'Must-Buy Section'-based methods.

This method also contains limitations. The first limitation is that the entire simulation will cost more computational time and resources than traditional parsing methods. Additionally, the cost of computational resources will significantly increase when they simulate.

Author Contributions: Y.H.: Supervision, Methodology, Investigation, and Software. S.G.: Conceptualization, Software, and Formal Analysis. Y.W.: Software and Writing—Review and Editing. Y.Z.: Software and Validation. W.Z.: Validation and Writing—Original Draft Preparation. F.X.: Supervision, Project Administration, and Mathematical Modeling. C.S.L.: Code Debugging, Visualization, and Formal Analysis. A.F.Z.: Visualization and Data Curation. All authors have read and agreed to the published version of the manuscript.

Appendix A

The specific parameters of Scenario 1 of the 9-bus system case are shown in Tables A1–A3. Compared with Scenario 1, Scenario 2 changes the PLmax of line 7 from 150 MW to 220 MW, no change in power producer parameters.

The specific parameters of Scenario 1 of the 33-bus system case are shown in Tables A4–A6. Compared with Scenario 1, Scenario 2 of the 33-bus system changes the PLmax of line 1 and line 2 from 150 MW to 250 MW, the PLmax of line 5, line 8, line 20, line 24, line 34, and line 36 from 100 MW to 150 MW, the PLmax of line 19 and line 20 from 150 MW to 200 MW, and the PLmax of line 22 from 100 MW to 200 MW. No change in power producer parameters.

Table A1. Bus system.

| | Basic Load (MW) | | | | | |
| | L1 | L2 | L3 | L4 | L5 | L6 |
Connected Bus	B1	B3	B4	B6	B7	B9
1 h	24.81	52.24	47.00	106.99	58.40	41.34
2 h	24.01	50.56	45.48	103.54	56.52	40.01
3 h	23.54	49.56	44.58	101.50	55.41	39.22
4 h	23.44	49.35	44.39	101.06	55.17	39.05
5 h	23.91	50.34	45.29	103.09	56.28	39.84
6 h	25.35	53.36	48.01	109.28	59.66	42.23
7 h	28.32	59.63	53.65	122.13	66.67	47.19
8 h	31.49	66.29	59.64	135.77	74.12	52.46
9 h	32.19	67.76	60.96	138.78	75.76	53.63
10 h	32.58	68.59	61.71	140.47	76.68	54.28
11 h	32.47	68.36	61.50	139.99	76.42	54.10
12 h	31.81	66.98	60.26	137.18	74.89	53.01
13 h	31.73	66.81	60.11	136.83	74.70	52.88
14 h	31.64	66.62	59.93	136.44	74.48	52.72
15 h	31.32	65.94	59.32	135.05	73.72	52.19
16 h	31.82	67.00	60.28	137.22	74.91	53.02
17 h	33.23	69.96	62.94	143.27	78.21	55.36
18 h	35.50	74.74	67.24	153.07	83.56	59.15
19 h	35.13	73.96	66.54	151.47	82.69	58.53
20 h	34.27	72.15	64.91	147.76	80.66	57.10
21 h	33.02	69.51	62.53	142.36	77.71	55.01
22 h	31.30	65.89	59.28	134.94	73.66	52.14
23 h	28.60	60.21	54.17	123.32	67.32	47.65
24 h	25.69	54.09	48.66	110.77	60.47	42.80

Table A2. Bidding parameters of power producers in the 9-bus system.

	Gmax (MW)	Gmin (MW)	Initial Status	Ramp	Initial Bidding Coefficient	A ($/MW^2)	B ($/MW)	C ($)	Startup Cost	Shutdown Cost
G1	300	20	1	220	1.05	0.0004	13.7	174.3	180	0
G2	250	20	1	100	1.05	0.005	17.6	137.4	60	0
G3	250	20	1	100	1.05	0.005	18.2	131.2	60	0

Table A3. Parameters of 9-bus system.

Item	Impedance (Ω)	PLmax (MW)
Lines_1 B1-B2	0.0576	100
Lines_2 B2-B3	0.092	180
Lines_3 B3-B4	0.17	120
Lines_4 B4-B5	0.0586	150
Lines_5 B5-B6	0.1008	160
Lines_6 B6-B7	0.072	140
Lines_7 B7-B8	0.0626	150
Lines_8 B8-B9	0.161	120
Lines_9 B9-B1	0.085	80
Lines_10 B9-B2	0.084	120
Lines_11 B7-B5	0.163	80

Table A4. Data of the base load in the 33-bus system.

	Basic Load (MW)						
	L1	**L2**	**L3**	**L4**	**L5**	**L6**	**L7**
Connected Bus	**B5**	**B7**	**B11**	**B20**	**B24**	**B29**	**B33**
1 h	71.99	49.61	99.95	92.76	83.44	113.60	87.04
2 h	69.67	48.01	96.73	89.77	80.75	109.94	84.23
3 h	68.29	47.06	94.82	88.00	79.16	107.77	82.57
4 h	68.01	46.86	94.42	87.62	78.82	107.31	82.22
5 h	69.37	47.80	96.32	89.39	80.40	109.47	83.87
6 h	73.54	50.68	102.10	94.75	85.23	116.04	88.91
7 h	82.18	56.63	114.10	105.89	95.25	129.68	99.36
8 h	91.36	62.96	126.84	117.72	105.89	144.17	110.45
9 h	93.39	64.35	129.66	120.33	108.24	147.37	112.94
10 h	94.53	65.14	131.24	121.80	109.56	149.16	114.28
11 h	94.20	64.92	130.79	121.38	109.19	148.65	113.89
12 h	92.31	63.61	128.16	118.94	106.99	145.66	111.60
13 h	92.08	63.45	127.84	118.64	106.72	145.30	111.32
14 h	91.81	63.27	127.47	118.30	106.41	144.88	111.00
15 h	90.88	62.62	126.17	117.09	105.33	143.40	109.87
16 h	92.34	63.63	128.20	118.97	107.02	145.70	111.63
17 h	96.41	66.44	133.86	124.23	111.74	152.14	116.56
18 h	103.01	70.98	143.01	132.72	119.39	162.54	124.53
19 h	101.99	70.24	141.52	131.33	118.14	160.84	123.23
20 h	99.43	68.52	138.05	128.11	115.24	156.90	120.21
21 h	95.79	66.01	133.00	123.43	111.03	151.16	115.81
22 h	90.80	62.57	126.07	117.00	105.24	143.29	109.78
23 h	82.98	57.18	115.21	106.92	96.18	130.95	100.32
24 h	74.54	51.37	103.49	96.04	86.39	117.62	90.12

Table A5. Bidding parameters of power producers in the 33-bus system.

	Gmax (MW)	Gmin (MW)	Initial Status	Ramp	Initial Bidding Coefficient	A ($/MW^2)	B ($/MW)	C ($)	Startup Cost	Shutdown Cost
G1	220	0	1	50	1.05	0.0004	15.5	176.9	180	0
G2	180	0	1	30	1.05	0.0045	18.1	168.4	180	0
G3	250	0	1	30	1.05	0.001	19.6	129.9	360	0
G4	150	0	1	25	1.05	0.005	17.6	137.4	60	0
G5	250	0	1	40	1.05	0.0047	20.2	130.6	60	0
G6	300	0	1	55	1.05	0.0026	17.2	137.8	60	0

Table A6. Parameters of the 33-bus system.

Item	Impedance (Ω)	PLmax (MW)
Lines_1 B1-B2	0.0470	150
Lines_2 B2-B3	0.2511	150
Lines_3 B3-B4	0.1864	100
Lines_4 B4-B5	0.1941	100
Lines_5 B5-B6	0.7070	100
Lines_6 B6-B7	0.6188	100
Lines_7 B7-B8	0.2351	100
Lines_8 B8-B9	0.7400	100
Lines_9 B9-B10	0.7400	100
Lines_10 B10-B11	0.0650	100
Lines_11 B11-B12	0.1238	100
Lines_12 B12-B13	1.1550	100
Lines_13 B13-B14	0.7129	100
Lines_14 B14-B15	0.5260	100
Lines_15 B15-B16	0.5450	200
Lines_16 B16-B17	1.7210	200
Lines_17 B17-B18	0.5740	200
Lines_18 B1-B19	0.1565	150
Lines_19 B19-B20	1.3554	150
Lines_20 B20-B21	0.4784	100
Lines_21 B21-B22	0.9373	100
Lines_22 B3-B23	0.3083	100
Lines_23 B23-B24	0.7091	200
Lines_24 B24-B25	0.7011	100
Lines_25 B6-B26	0.1034	150
Lines_26 B26-B27	0.9337	200
Lines_27 B27-B28	0.1447	200
Lines_28 B28-B29	0.7006	200
Lines_29 B29-B30	0.2585	100
Lines_30 B30-B31	0.9630	100
Lines_31 B31-B32	0.3619	100
Lines_32 B32-B33	0.5362	100
Lines_33 B8-B21	0.6842	100
Lines_34 B9-B15	0.9524	100
Lines_35 B12-B22	0.8661	100
Lines_36 B25-B29	0.7216	100
Lines_37 B33-B18	0.5641	250

Appendix B

The parameters of the power producer and the line in the 6-bus system are the same, but Scenario 1 does not add any price boundaries, and Scenario 2 sets the maximum bidding coefficient for power producer 1 to 1.5.

Table A7. Data of the base load in the 6-bus system.

	Basic Load (MW)		
	L1	L2	L3
Connected Bus	B1	B3	B4
1 h	60.95	52.28	42.70
2 h	58.98	50.60	41.33
3 h	57.82	49.60	40.51
4 h	57.57	49.38	40.34
5 h	58.73	50.38	41.15
6 h	62.26	53.40	43.62
7 h	69.57	59.68	48.75
8 h	77.34	66.34	54.19

Table A7. *Cont.*

	Basic Load (MW)		
	L1	**L2**	**L3**
Connected Bus	**B1**	**B3**	**B4**
9 h	79.06	67.82	55.10
10 h	80.02	68.64	56.07
11 h	79.75	68.41	55.88
12 h	78.15	67.03	54.76
13 h	77.95	66.86	54.62
14 h	77.72	66.67	54.46
15 h	76.93	65.99	53.90
16 h	78.17	67.05	54.77
17 h	81.62	70.01	57.19
18 h	87.20	74.80	61.10
19 h	86.29	74.02	60.46
20 h	84.17	72.20	58.98
21 h	81.10	69.56	56.82
22 h	76.87	65.94	53.86
23 h	70.25	60.26	49.22
24 h	63.10	54.13	44.22

Table A8. Bidding parameters of power producers in the 6-bus system.

	Gmax (MW)	Gmin (MW)	Initial Status	Ramp	Initial Bidding Coefficient	A ($/MW^2)	B ($/MW)	C ($)	Startup Cost	Shutdown Cost
G1	250	0	1	50	1.05	0.0004	13.5	176.9	180	0
G2	200	0	1	30	1.05	0.0006	16.9	146.4	60	0

Table A9. Parameters of the 6-bus system.

Item	Impedance (Ω)	PLmax (MW)
Lines_1 B1-B2	0.2304	80
Lines_2 B2-B3	0.0920	100
Lines_3 B3-B4	0.6802	80
Lines_4 B4-B5	0.1327	100
Lines_5 B5-B6	0.0567	100
Lines_6 B6-B1	0.1333	100
Lines_7 B6-B3	0.0626	100

References

1. Bhattacharya, K.; Bollen, M.H.J.; Daalder, J.E. *Operation of Restructured Power Systems*; Springer Science & Business Media: Berlin/Heidelberg, Germany, 2012.
2. Wilson, J.D.; O'Boyle, M.; Lehr, R. Monopsony behavior in the power generation market. *Electr. J.* **2020**, *33*, 106804. [CrossRef]
3. Yokoyama, R.; Oyama, T.; Yorino, N.; Ishikawa, T.; Mori, H.; Hiyama, T. Advanced and intelligent technologies for reliable operation of power systems and electricity markets. *IEEJ Trans. Electr. Electron. Eng.* **2008**, *3*, 464–472. [CrossRef]
4. Mohd Isa, A.; Niimura, T.; Yokoyama, R. Multicriteria transmission congestion management by load curtailment and generation redispatch in a deregulated power system. *IEEJ Trans. Electr. Electron. Eng.* **2008**, *3*, 524–529. [CrossRef]
5. Zhong, J. *Power System Economic and Market Operations*; CRC Press: Boca Raton, FL, USA, 2018.
6. Makkonen, M.; Pätäri, S.; Jantunen, A.; Viljainen, S. Competition in the European electricity markets—Outcomes of a Delphi study. *Energy Policy* **2012**, *44*, 431–440. [CrossRef]
7. Ribó-Pérez, D.; Van der Weijde, A.H.; Álvarez-Bel, C. Effects of self-generation in imperfectly competitive electricity markets: The case of Spain. *Energy Policy* **2019**, *133*, 110920. [CrossRef]
8. Nepal, R.; Carvalho, A.; Foster, J. Revisiting electricity liberalization and quality of service: Empirical evidence from New Zealand. *Appl. Econ.* **2016**, *48*, 2309–2320. [CrossRef]
9. Ghazvini, M.A.F.; Canizes, B.; Vale, Z.; Morais, H. Stochastic short-term maintenance scheduling of GENCOs in an oligopolistic electricity market. *Appl. Energy* **2013**, *101*, 667–677. [CrossRef]

10.　Ding, J.; Xu, Y.; Chen, H.; Sun, W.; Hu, S.; Sun, S. Value and economic estimation model for grid-scale energy storage in monopoly power markets. *Appl. Energy* **2019**, *240*, 986–1002. [CrossRef]

11.　Bushnell, J.; Knittel, C.R.; Wolak, F. Estimating the opportunities for market power in a deregulated Wisconsin electricity market. *J. Ind. Econ.* **1999**, *47*.

12.　Shahidehpour, M.; Alomoush, M. *Restructured Electrical Power Systems: Operation, Trading, and Volatility*; CRC Press: Boca Raton, FL, USA, 2017.

13.　Wolfram, C. *Strategic Bidding in a Multi-Unit Auction: An Empirical Analysis of Bids to Supply Electricity*; Working Paper 6269; National Bureau of Economic Research: Cambridge, MA, USA, 1997.

14.　Hesamzadeh, M.R.; Biggar, D.R.; Hosseinzadeh, N. The TC-PSI indicator for forecasting the potential for market power in wholesale electricity markets. *Energy Policy* **2011**, *39*, 5988–5998. [CrossRef]

15.　Arellano, M.S.; Serra, P. The competitive role of the transmission system in price-regulated power industries. *Energy Econ.* **2008**, *30*, 1568–1576. [CrossRef]

16.　Haas, R.; Auer, H. The prerequisites for effective competition in restructured wholesale electricity markets. *Energy* **2006**, *31*, 857–864. [CrossRef]

17.　Lee, Y.Y.; Baldick, R.; Hur, J. Firm-based measurements of market power in transmission-constrained electricity markets. *IEEE Trans. Power Syst.* **2011**, *26*, 1962–1970. [CrossRef]

18.　Wang, P.; Xiao, Y.; Ding, Y. Nodal market power assessment in electricity markets. *IEEE Trans. Power Syst.* **2004**, *19*, 1373–1379. [CrossRef]

19.　Aliabadi, D.E.; Kaya, M.; Şahin, G. An agent-based simulation of power generation company behavior in electricity markets under different market-clearing mechanisms. *Energy Policy* **2017**, *100*, 191–205. [CrossRef]

20.　Macal, C.; Thimmapuram, P.; Koritarov, V.; Koritarov, V.; Conzelmann, G.; Veselka, T.; North, M.; Mahalik, M.; Botterud, A.; Cirillo, R. Agent-based simulation of electric power markets. In Proceedings of the Winter Simulation Conference 2014, Savannah, GA, USA, 7–10 December 2014; pp. 276–287.

21.　Kiran, P.; Chandrakala, K.R.M.V. New interactive agent based reinforcement learning approach towards smart generator bidding in electricity market with micro grid integration. *Appl. Soft Comput.* **2020**, *97*, 106762.

22.　Li, G.; Shi, J. Agent-based simulation for trading wind power with uncertainty in the day-ahead wholesale electricity markets of single-sided auctions. *Appl. Energy* **2012**, *99*, 13–22. [CrossRef]

23.　Viehmann, J.; Lorenczik, S.; Malischek, R. Multi-unit multiple bid auctions in balancing markets: An agent-based Q-learning approach. *Energy Econ.* **2021**, *93*, 105035. [CrossRef]

24.　Ye, Y.; Qiu, D.; Papadaskalopoulos, D.; Strbac, G. A deep Q network approach for optimizing offering strategies in electricity markets. In Proceedings of the 2019 International Conference on Smart Energy Systems and Technologies (SEST), Porto, Portugal, 9–11 September 2019; pp. 1–6.

25.　Mohtavipour, S.S.; Zideh, M.J. An iterative method for detection of the collusive strategy in prisoner's dilemma game of electricity market. *IEEJ Trans. Electr. Electron. Eng.* **2019**, *14*, 252–260. [CrossRef]

26.　Brooks, A.E.; Lesieutre, B.C. A locational marginal price for frequency balancing operations in regulation markets. *Appl. Energy* **2022**, *308*, 118306. [CrossRef]

27.　Hu, B.; Wu, L.; Guan, X.; Gao, F.; Zhai, Q. Comparison of variant robust SCUC models for operational security and economics of power systems under uncertainty. *Electr. Power Syst. Res.* **2016**, *133*, 121–131. [CrossRef]

28.　Dai, C.; Wu, L.; Wu, H. A multi-band uncertainty set based robust SCUC with spatial and temporal budget constraints. *IEEE Trans. Power Syst.* **2016**, *31*, 4988–5000. [CrossRef]

29.　Xu, F.Y.; Tang, R.X.; Xu, S.B.; Fan, Y.; Zhou, Y.; Zhang, H.A. Neural network-based photovoltaic generation capacity prediction system with benefit-oriented modification. *Energy* **2021**, *223*, 119748. [CrossRef]

30.　Jaghargh, M.J.P.; Mashhadi, H.R. An analytical approach to estimate structural and behavioral impact of renewable energy power plants on LMP. *Renew. Energy* **2021**, *163*, 1012–1022. [CrossRef]

31.　Alabdullah, M.H.; Abido, M.A. Microgrid energy management using deep Q-network reinforcement learning. *Alex. Eng. J.* **2022**, *61*, 9069–9078. [CrossRef]

32.　Kosana, V.; Teeparthi, K.; Madasthu, S.; Kumar, S. A novel reinforced online model selection using Q-learning technique for wind speed prediction. *Sustain. Energy Technol. Assess.* **2022**, *49*, 101780. [CrossRef]

33.　Russell, S.; Norvig, P. *Artificial Intelligence: A Modern Approach*; Pearson: Upper Saddle River, NJ, USA, 2002.